ELSEVIER

Chemical Engineering Journal 137 (2008) 339–346

Chemical Engineering Journal

www.elsevier.com/locate/cej

Optimal design of complex manifold geometries for uniform flow distribution between microchannels

Minqiang Pan *, Yong Tang, Liang Pan, Longsheng Lu

School of Mechanical Engineering, South China University of Technology, Guangzhou 510640, PR China

Received 8 June 2006; received in revised form 26 March 2007; accepted 2 May 2007

Abstract

The objective of this work is to study the influence of complex manifold geometries on the flow distribution between microchannels by an analytical model and an equivalent electrical resistance network model. An optimization procedure is proposed to optimize the manifold geometries and dimensional variations to obtain comparatively ideal flow distribution between microchannels. A specific case is illustrated by applying the proposed optimization procedure to analyze the optimal rules for a given inlet distributing manifold geometry. Result shows that the microchannel width dominates the optimization of outlet collecting manifold geometry and dimensional variations.

Keywords: Complex manifold geometry; Microchannel; Flow distribution

1. Introduction

Microchannel reactors are three-dimensional structural components with microchannels, which are manufactured on solid materials by microfabrication technology. The incorporation of microchannels, with characteristic dimensions on the order of hundreds of microns, into the microreactors, offers higher heat and mass transfer rates, as well as higher surface-to-volume ratios, leading to improved reaction efficiency and smaller reaction volumes. Moreover, microchannels exhibit few risks because the flame is almost extinguished within the small dimensions, providing safe operation in the range of explosion without any special safety measure [1,2].

Introducing a single microchannel into the microreactor only serves a single reaction, and therefore it is hard to satisfy actual reaction requirements. Incorporating parallel microchannel arrays into microreactors can integrate not only complicated system with multiple reactions, but also enable the coupling of endothermic and exothermic reactions, which makes full use of the waste heat. Currently, parallel microchannel arrays have been successfully applied into several microreactors, such as compact fuel processors for producing hydrogen [3], CO preferential oxidation microreactors [4], micro heat exchangers [5] and micromixers [6].

The geometrical structure of the manifolds and microchannels play an important role in the flow distribution between microchannels, which affects the heat and mass transfer efficiency, even the performance of microreactors [7]. Therefore the geometrical design of manifolds and microchannels is one of the important design factors to be considered. Current geometrical design largely depends on the rule of thumb, although there have been a few related researches which mainly focused on studying the optimal design of simple manifold geometries for uniform flow distribution between microchannels. Commenge et al. [7] found that when the wall of inlet distributing chamber was regular, a slight curvature could appear along the wall of output collecting chamber if flow uniformity was to be realized between microchannels. Tonomura et al. [8] studied the effects of rectangular manifolds on the flow distribution between microchannels of plate-fin microdevices by CFD simulation.

The advances in microfabrication technology not only make it possible to fabricate complex manifold geometries, but also offer much higher production efficiency and lower cost. Therefore complex manifold geometries could be extensively applied into microreactors gradually. The optimal design of complex manifold geometries for flow uniformity between microchannels becomes more important since simple manifold geometries belong to a special case of complex manifold geometries.

* Corresponding author. Tel.: +86 20 8711 4634; fax: +86 20 8711 4634.
E-mail address: vikypan@sina.com (M. Pan).

1385-8947/$ – see front matter © 2007 Elsevier B.V. All rights reserved.
doi:10.1016/j.cej.2007.05.012

Nomenclature

A	sectional area of rectangular channel (m^2)
D_H	hydraulic nominal diameter (m)
E	microchannel depth (m)
F	function
IDM	inlet distributing manifold
L	length of manifold (m)
N	microchannel number
OCM	outlet collecting manifold
ΔP	pressure drop (Pa)
Q_T	total feed flow rate (m^3/s)
$Q(j)$	flow rate of the jth channels (m^3/s)
$R(j)$	flow resistance of the jth channels (Pa s/m^3)
S	area ratio of IDM and OCM
U	fluid velocity (m/s)
W	channel width (m)
$W(j)$	width of jth channels (m)
X	horizontal ordinate of manifold (m)

Subscripts

c	microchannel
in	inlet distributing manifold
out	outlet collecting manifold

Greek letters

λ_{NC}	non-circular coefficient
μ	viscosity (kg/ms)

The objective of this work is to study the influence of complex manifold geometries on the flow distribution between microchannels by an analytical model and an equivalent electrical resistance network model. An optimization procedure is proposed to optimize the manifold geometries and dimensional variations to obtain comparatively ideal flow distribution between microchannels. A specific case is illustrated by applying the proposed optimization procedure to analyze the optimal rules for a given inlet distributing manifold geometry.

2. Complex manifold geometry

2.1. Description of the model studied

Generally endothermic and exothermic reactions are coupled in the microreactors to improve energy recycle and reduce thermal loss. Although the symmetric manifold geometries are theoretically in favor of achieving ideal flow uniformity between microchannels, the manifold geometry should deviate to one side and leave other side as a flow passage for the other fluid to make two fluids alternately flow between each other to exchange heat, as shown in Fig. 1.

The model studied here consists of an inlet distributing manifold (IDM), parallel microchannels and an outlet collecting manifold (OCM), as shown in Fig. 2. The geometries of IDM and OCM are curved side trapezoids, that is, three edges are straight lines, two of them are parallel to each other, and the third one is perpendicular to them; the forth edge is curve. The inlet and outlet of fluid are perpendicular to one side of the IDM and OCM, respectively. The flow pattern of fluid is a *Z*-shape where the outlet flows in the same direction as the inlet flows.

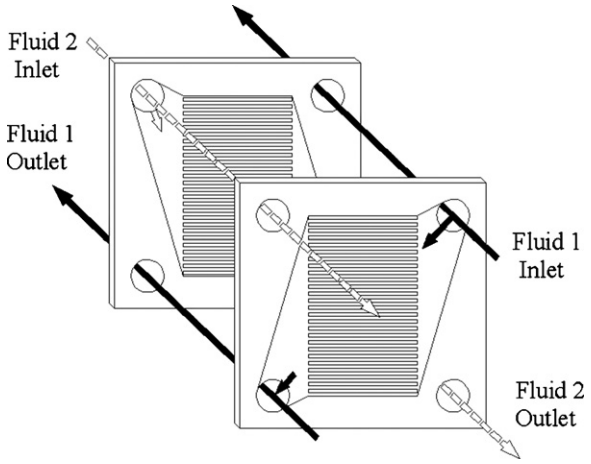

Fig. 1. The structure that realizes two fluids alternately flow.

2.2. Analytical model

The curves of IDM and OCM are assumed to be continuous equations $W_{in}(j) = F_1[X_{in}(j)]$ and $W_{out}(j) = F_2[X_{out}(j)]$, respectively. Since one edge of the manifolds is curve, it is difficult to study the condition of the fluid in the manifolds by preliminary mathematics. But $F_1[X_{in}(j)]$ and $F_2[X_{out}(j)]$ are continuous, they both have little changes in a small zone and can be regard as changeless. Therefore, IDM and OCM are divided into N mean zones, respectively, then the values of $F_1[X_{in}(j)]$ and $F_2[X_{out}(j)]$ in each zone are chosen as the depth for rectangles, which forms N rectangular channels. Since the intervals between the microchannels are pretty small, the sum of the N rectangular channels can be regarded as the area of the manifold, as shown in Fig. 3. The length of each rectangular channel is L/N, and the width of each rectangular channel is $F_1[X_{in}(j)]$ and $F_2[X_{out}(j)]$, respectively. Certainly, there are some errors between the analytical model and the actual manifolds, but the practical microchannel number is adequately large, which results in comparatively small errors.

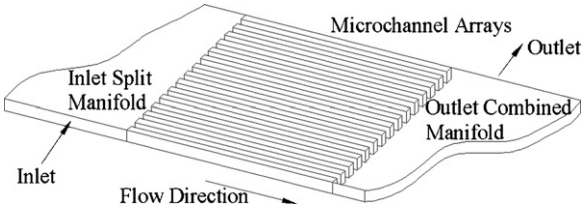

Fig. 2. The model studied in this work.

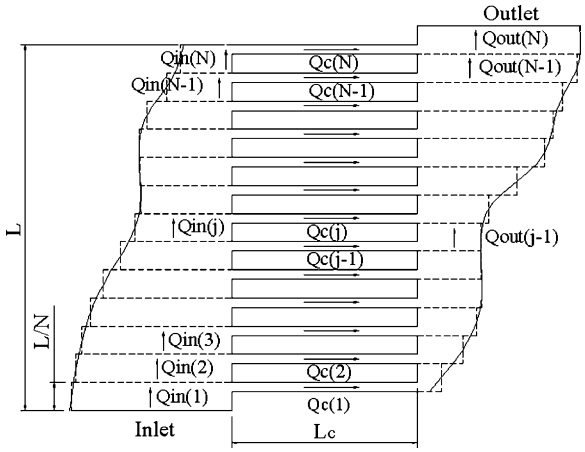

Fig. 3. Analytical model.

3. Mathematical model

3.1. Pressure drop through rectangular channels

In practice, flow velocities in microchannels are usually lower than 10 m/s and the hydraulic diameters are no more than 500 μm, so the Reynolds number is lower than 2000. Therefore flow pattern on the microscale is considered as laminar, and fluid is considered as incompressible and continuum in the analysis.

Three kinds of important resistances exist during flowing in microchannel arrays: (a) the local resistances caused by splitting and turning when the fluid flows from IDM to microchannel arrays; (b) the frictional resistances caused by friction effects during flowing inside microchannel arrays; (c) the local resistances caused by combining and turning as the fluid flows from microchannel arrays to OCM. Researches [9] indicated that the magnitudes of local resistances in microchannel arrays are much lower than that of frictional ones, and the neglect of local resistances can simplify the algorithm of microchannel array model [7,10], therefore local resistances are ignored in this study.

The purpose of dividing the manifold into N rectangular channels in same length and different width in the analytical model is to analyze the relationship between pressure drop and flow distribution by Hagen–Poiseuille Equation of rectangular channels. For laminar flow, the relation between pressure drop ΔP and flow rate Q through rectangular channels is defined below:

$$\Delta P = \frac{32\mu L\lambda_{NC}}{D_H^2}U = \frac{32\mu L\lambda_{NC}}{D_H^2 A}Q \tag{1}$$

where D_H is hydraulic nominal diameter, $D_H = 2WE/(W+E)$; A the sectional area of rectangular channel, $A = WE$; λ_{NC} the non-circular coefficient [7,10], and $\lambda_{NC} = (3/2)/[(1-0.351(E/W))^2(1+E/W)^2]$ when $0 \le E/W \le 1$, or else, E/W is substitute for W/E when $E/W > 1$. Here, the microchannel depth E is assumed to be less than the width W.

3.2. Equivalent electrical resistance network model

In order to distinctly analyze the relation between pressure drop ΔP, flow rate Q and flow resistance R, the analytical model is simplified by an equivalent electrical resistance network model, as depicted in Fig. 4. In this model, the microchannels, and the rectangular channels of IDM and OCM are replaced by electrical resistance. Pressure drop ΔP through the rectangular channel is represented as the potential difference through the electrical resistance, flow rate Q and flow resistance R are equivalent to current and electrical resistance, respectively. Similar to Ohm's law, the relationship of pressure drop ΔP, flow rate Q and flow resistance R is defined as follows:

$$\Delta P = RQ \tag{2}$$

where the flow resistance R is defined as

$$R = \frac{32\mu L\lambda_{NC}}{D_H^2 A} \tag{3}$$

According to Eq. (1), R can be written in another form as

$$R = \frac{12\mu L}{(1-0.351(E/W))^2 WE^3} \tag{4}$$

The rectangular channels of IDM and OCM are numbered up from 1st to Nth, respectively. The equivalent electrical resistance network model consists of $N-1$ loops. The pressure drop of two ends in the diagonal line of each loop via two different flow channels are equal [10], therefore $N-1$ equations can be expressed as follows:

$$R_{in}(j)Q_{in}(j) + R_c(j)Q_c(j) = R_{out}(j-1)Q_{out}(j-1) + R_c(j-1)Q_c(j-1) \quad (j = 2, 3, \ldots, N) \tag{5}$$

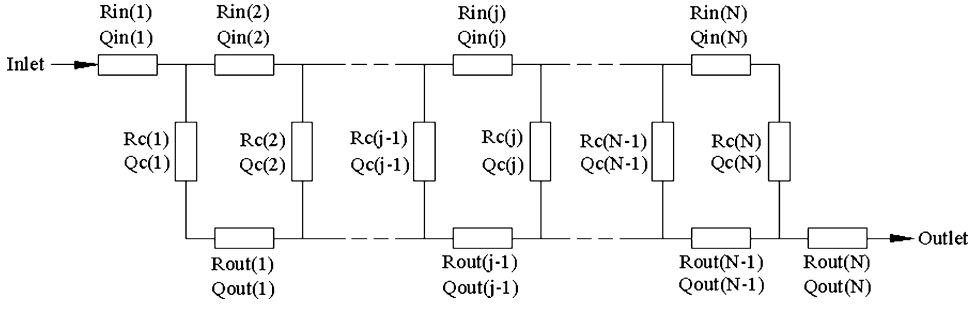

Fig. 4. Equivalent electrical resistance network model.

The relation between the flow rate in each rectangular channel of IDM and microchannel is defined as follows:

$$Q_{in}(j) = Q_c(j) + Q_{in}(j+1) \quad (j = 1, 2, \ldots, N-1) \tag{6}$$

$$Q_{in}(1) = Q_T \tag{7}$$

$$Q_{in}(N) = Q_c(N) \tag{8}$$

where Q_T is the total feed flow rate.

The relation between the flow rate in each rectangular channel of OCM and microchannel is defined as follows:

$$Q_{out}(j) = Q_c(j) + Q_{out}(j-1) \quad (j = 2, 3, \ldots, N) \tag{9}$$

$$Q_{out}(N) = Q_T \tag{10}$$

If the dimensional variations of channels were given, the resistance of each channel $R_{in}(j)$, $R_c(j)$, $R_{out}(j)$ can be calculated by Eq. (4). There are $3N$ variables in the equivalent electrical resistance network, and there are $3N$ equations from Eqs. (5)–(10), therefore the flow rate in each channel can be solved by Eqs. (5)–(10).

3.3. Solution algorithm

Parallel microchannels are generally manufactured by microfabrication technology, such as laser ablation or chemical etching, ensuring that each microchannel has the same characteristic dimensions, such as length, width and depth. Therefore the resistance of each microchannel is equal, i.e.

$$R_c(j) = R_c(j-1) \tag{11}$$

Although the flow rate of each microchannel can be calculated by Eqs. (5)–(10), when all the dimensional variations of the analytical model are given, uniform flow distribution between microchannels is always hard to achieve, Therefore, it is assumed that the flow rate of each microchannel is equal, and then, under this assumption, the dimensional variations of the model can be worked out.

Equal flow rate of each microchannel can be expressed as follows:

$$Q_c(j) = Q_c(j-1) = \frac{1}{N} Q_T \quad (j = 2, 3, \ldots, N) \tag{12}$$

So the following equations are obtained:

$$Q_{in}(j) = Q_{in}(1) - \sum_{k=1}^{j-1} Q_c(k) = \frac{N-(j-1)}{N} Q_T \tag{13}$$

$$Q_{out}(j-1) = \sum_{k=1}^{j-1} Q_c(k) = \frac{j-1}{N} Q_T \tag{14}$$

Substituting Eqs. (4), (12), (13) and (14) into Eq. (5), the following equation can be obtained:

$$\frac{N-j+1}{j-1} = \frac{[1-0.351(E/W_{in}(j))]^2 W_{in}(j)}{[1-0.351(E/W_{out}(j-1))]^2 W_{out}(j-1)} \quad (j = 2, 3, \ldots, N) \tag{15}$$

Eq. (15) indicates the necessary relation between the width $W_{in}(j)$ of jth rectangular channel of IDM and $W_{out}(j-1)$ of $(j-1)$th rectangular channel of OCM if the uniform flow distribution between microchannels needs to be achieved. When the curve equation $W_{in}(j) = F_1[X_{in}(j)]$ of IDM is given, the curve equation $W_{out}(j-1) = F_2[X_{out}(j-1)]$ of OCM can be deduced by calculating the width of each rectangular channel of OCM and vice versa. It should be noted that the width W_1 of IDM and W_N of OCM do not appear in the Eq. (15). However, they can be solved by fitting the curve of IDM and OCM.

4. Analysis of special case

It indicates that the dimensional variations appearing in the Eq. (15) determine the flow distribution between microchannels. These dimensional variations are the width of each rectangular channel $W_{in}(j)$ and $W_{out}(j-1)$, the microchannel number N and the microchannel depth E.

$W_{in}(j)$ and $W_{out}(j-1)$ depend on the curve equation $W_{in}(j) = F_1[X_{in}(j)]$ and $W_{out}(j-1) = F_1[X_{out}(j-1)]$, respectively, as well as the horizontal ordinate $X_{in}(j)$ and $X_{out}(j-1)$. $X_{in}(j)$ and $X_{out}(j-1)$ are defined as follows:

$$X_{in}(j) = j\frac{L}{N} \quad (j = 1, 2, \ldots, N-1) \tag{16}$$

$$X_{out}(j-1) = (j-1)\frac{L}{N} \quad (j = 2, 3, \ldots, N) \tag{17}$$

Therefore, besides the curve equations, $W_{in}(j)$ and $W_{out}(j-1)$ depend on the dimensional variations N and L. Then, the dimensional variations influencing on the flow distribution are changed for N, L and E.

To simplify the optimization algorithm, the width of the space between microchannels is assumed to be equal to that of microchannels, so the relation of L and W_c is defined as:

$$L = (2N-1)W_c \tag{18}$$

Then, the dimensional variations are changed with N, W_c and E.

However, it is hard to analyze the influence of dimensional variations on the flow distribution between microchannels by Eq. (15), except if one of the curve equations of two manifolds is given. In this paper, a specific curve equation of IDM is given, the OCM geometry and dimensional variations are optimized by a proposed optimization procedure, and the influence factor of the optimization process will be discussed.

4.1. Establishment of coordinate systems

Two coordinate systems are established to facilitate calculations of $W_{in}(j)$ and $W_{out}(j-1)$, as shown in Fig. 5. The left lower point of IDM is chosen as the origin of the coordinate system of the equation $W_{in}(j) = F_1[X_{in}(j)]$. The bottommost line segment of IDM is selected as the axis X and right as positive, while the leftmost line segment is selected as axis W and up as positive. The left upper point of OCM is chosen as the origin of the coordinate system of the equation $W_{out}(j-1) = F_2[X_{out}(j-1)]$. The

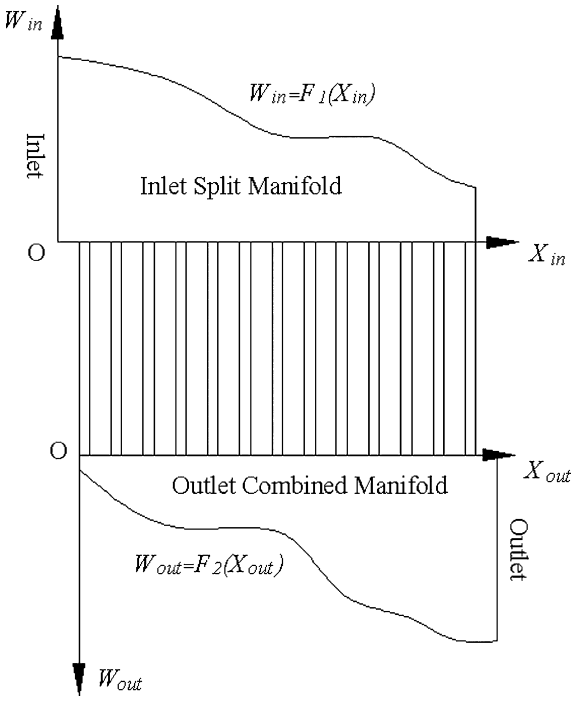

Fig. 5. The geometry of coordinate systems.

upmost line segment of OCM is selected as axis X and right as positive, while the leftmost line segment is selected as axis W and down as positive.

4.2. Optimization criterion

When the curve equation of IDM is given, a large number of OCM geometries are generated by Eq. (15) for different values of N, W_c and E. Therefore, it is necessary to establish effective criterion to get the optimal design.

When the curve equation of IDM is given, the curve may become non-monotonic with increasing number of microchannel number N (larger X value). Non-monotonic curve geometry results in dead volume [8], which is harmful for the flow of fluid, as shown in Fig. 6. Therefore, assuring that the curves of IDM and OCM are monotonic becomes the foremost optimization criterion.

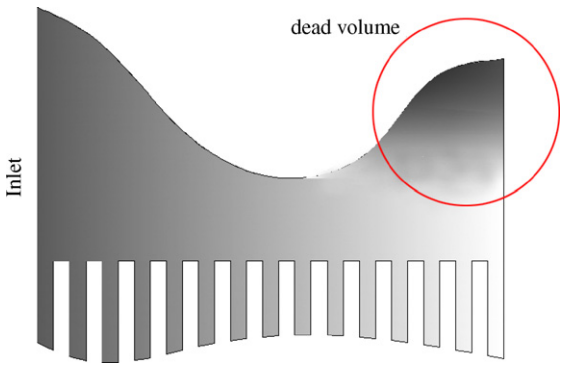

Fig. 6. Dead volume appears in the non-monotonic manifold curve.

Here, $W_{in}(j)=F_1[X_{in}(j)]$ is assumed to be a monotonic increasing function and $W_{out}(j-1)=F_2[X_{out}(j-1)]$ to be a monotonic decreasing function. In order to obtain monotonic curve, two requested optimization criterions are defined below:

$$W_{in}(j) > W_{in}(j+1) \tag{19}$$

$$W_{out}(j) < W_{out}(j+1) \tag{20}$$

Besides the restriction of monotony of manifold geometries, the area ratio of two manifolds needs to be restricted to avoid that one manifold is too large and the other is too small. The areas of IDM and OCM can be calculated by the sum of the rectangular channels, which are defined as follows:

$$S_{in} = \sum_{j=1}^{N-1} X_{in}(j) \times W_{in}(j) \tag{21}$$

$$S_{out} = \sum_{j=2}^{N} X_{out}(j) \times W_{out}(j) \tag{22}$$

The area ratio S of IDM to OCM which provides a comparison between the areas of two manifolds, is defined by the equation:

$$S = \left| \frac{S_{in}}{S_{out}} - 1 \right| \tag{23}$$

The objective of the second optimization criterion is to minimize the value of S.

4.3. Optimization procedure

It requires nevertheless lengthy time to reach the optimal design by manual calculation with the given curve equation $W_{in}=F_1(X_{in})$ of IDM. Therefore, an optimization procedure is proposed for efficient design. Fig. 7 shows the flowchart of the optimization procedure. In this developed method, the curve equation of IDM is given in advance, and then the microchannel width W_c (or depth E) is manually adjusted, while other dimensional variations are automatically optimized based on the optimization criterions until the optimal design is achieved. Two control parameters K and min S are defined for obtaining the minimal value of S.

5. Results and discussion

The given curve equation of IDM is defined below:

$$W_{in}(j) = \frac{1}{5}[X_{in}(j) - 8]^2 + 1 \quad (j = 1, 2, \ldots, N-1) \tag{24}$$

The width W_c and depth E of microchannel are independently manually adjusted to study their influences on the geometries of IDM and OCM, as well as other dimensional variations.

5.1. Influence of the microchannel width W_c

For the given curve equation of IDM, the microchannel width W_c is manually adjusted, while the microchannel depth E and microchannel number N are automatically optimized. Fig. 8

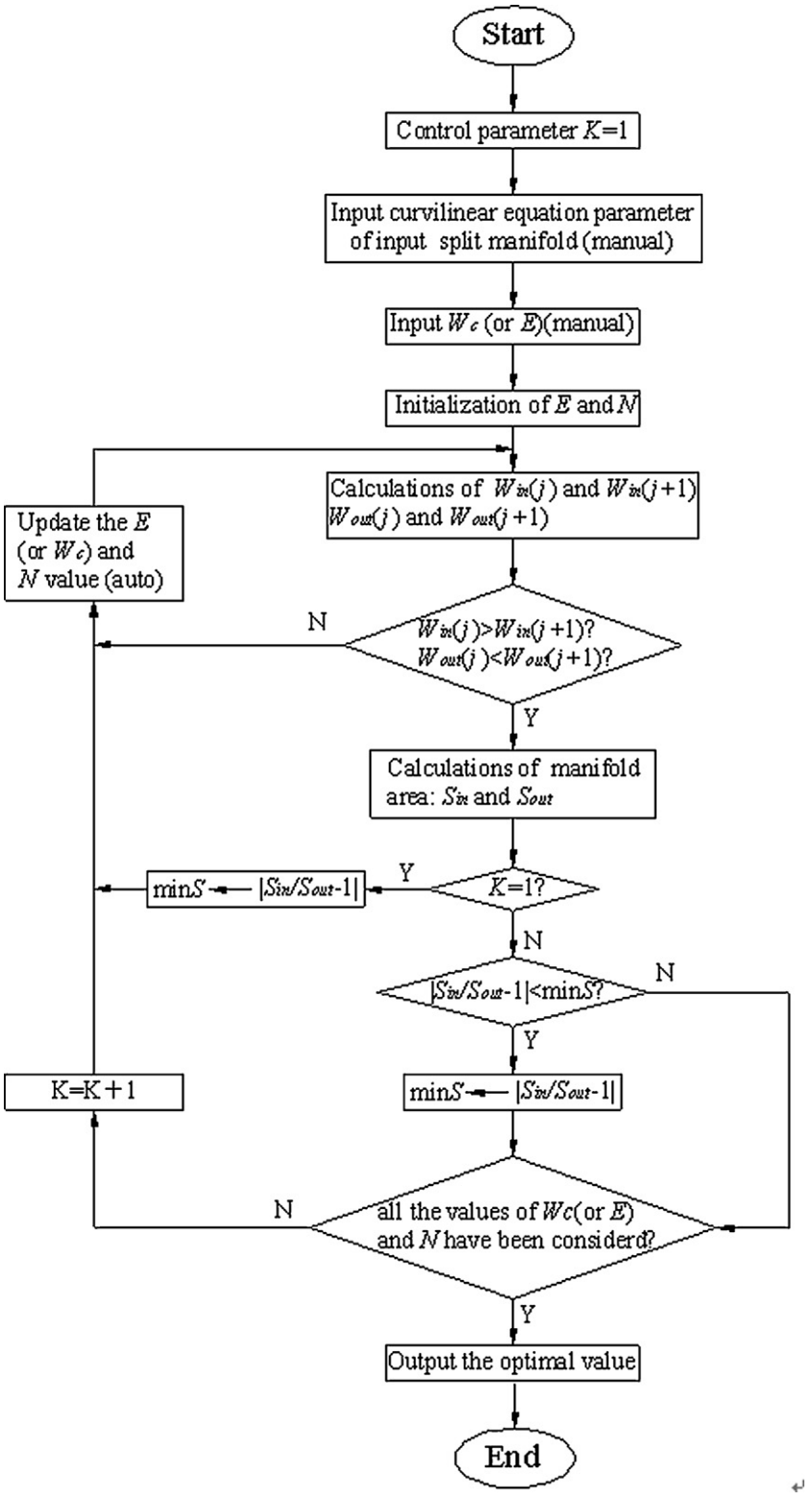

Fig. 7. The flowchart of the optimization procedure.

shows results for seven different W_c from 200 to 500 μm. The optimal OCM geometry is comparatively smooth when W_c is between 300 and 500 μm. The geometry becomes smoother with larger W_c, which favors fluid flow. However, small W_c produces steep geometry and small microchannel number N, which isn't suitable for practice. From the optimal results, E becomes larger with larger W_c, and at the same time the microchannel number N becomes comparatively larger.

Result in Fig. 9 demonstrates how the microchannel width W_c affects the IDM geometry. The trends are similar in all cases:

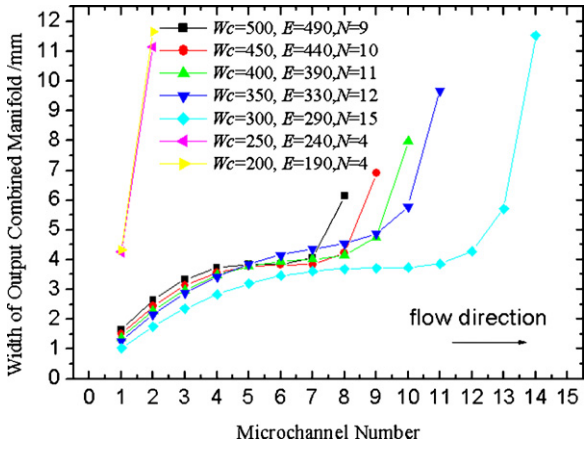

Fig. 8. The influence of W_c on the OCM geometry.

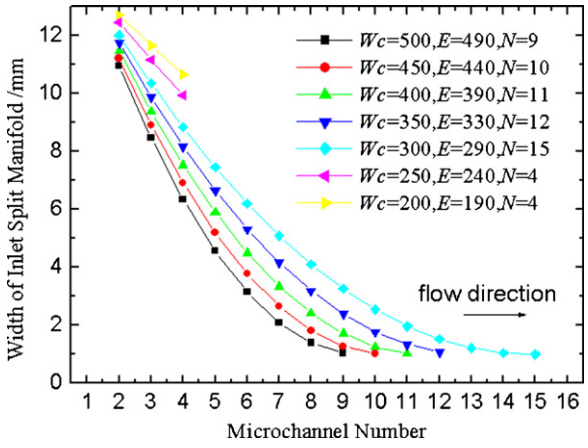

Fig. 9. The influence of W_c on the IDM geometry.

the IDM geometries are smoothly reduced. According to Eqs. (16) and (22), L changes with the varied W_c, resulting in the change of $X_{in}(j)$, therefore small variety of W_c lead to small variety of $X_{in}(j)$, the IDM geometry changes slightly. However, too small W_c leads to small microchannel number N, and the IDM geometry becomes too narrow for application.

Fig. 10 demonstrates the relation between the microchannel width W_c and the area ratio S of two manifolds. Result shows

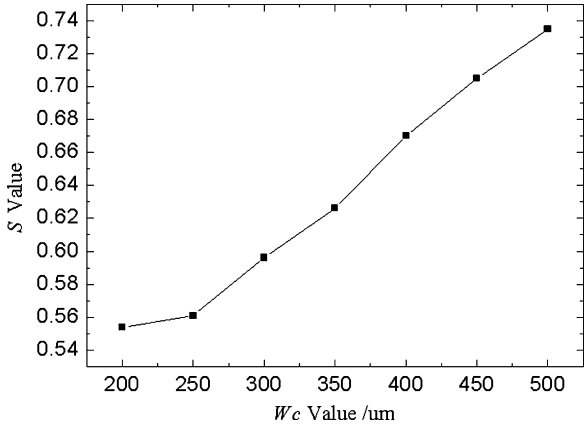

Fig. 10. Relation between W_c and S.

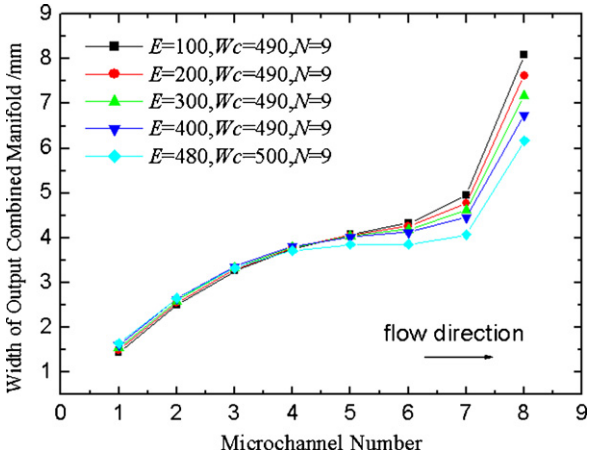

Fig. 11. The influence of E on the OCM geometry.

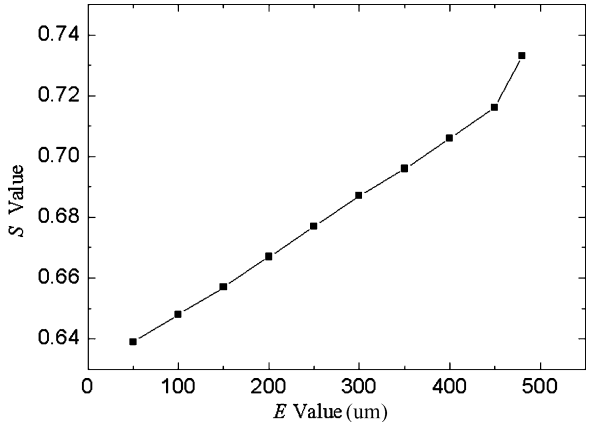

Fig. 12. Relation between E and S.

that S increases with the increasing W_c. The maximum value of S is 0.735, when W_c is 500 μm.

5.2. Influence of the microchannel depth E

In order to study the influence of the microchannel depth E on the OCM geometry and other dimensional variations, E is manually adjusted while W_c and N are automatically optimized. Fig. 11 visualizes the influences of E with five different values. Result shows that all the OCM geometries are almost consistent with each other. W_c and the OCM geometry change little with the changed E. According to Eq. (22), IDM geometry has nothing to do with E, therefore there is no influence of E on the IDM geometry.

Fig. 12 shows the relation between the microchannel depth E and the area ratio S of two manifolds. It shows that the area ratio of two manifolds becomes bigger with the larger E.

6. Conclusions

The problems of flow distribution between microchannels in the microreactors are studied. The influence of complex manifold geometries on the flow distribution between microchannels is analyzed by a proposed analytical model and an equivalent

electrical resistance network model. An optimization procedure is developed to optimize the manifold geometries and dimensional variations to obtain comparatively ideal flow distribution between microchannels.

A specific case is illustrated by applying the proposed optimization procedure to analyze the optimal rules for a given IDM geometry. Result shows that the division of the manifold into N rectangular channels is a valid method, and the microchannel width W_c dominates the optimization of OCM geometry and dimensional variations.

Acknowledgments

We extend our sincere thanks to the support of the National Nature Science Foundation of China, Project No. 50436010 and No. 50675070, and Guangzhou Key Project of Science and Technology, Project No. 2005Z2-D0011.

References

[1] D.G. Norton, E.D. Wetzel, D.G. Vlachos, Fabrication of single-channel catalytic microburners: effect of confinement on the oxidation of hydrogen/air mixtures, Ind. Eng. Chem. Res. 43 (2004) 4833–4840.

[2] P. Pfeifer, K. Schubert, G. Emig, Preparation of copper catalyst washcoats for methanol steam reforming in microchannels based on nanoparticles, Appl. Catal., A: Gen. 286 (2005) 175–185.

[3] G.G. Park, S.D. Yima, Y.G. Yoon, W.Y. Lee, C.S. Kima, D.J. Seo, K. Eguchi, Hydrogen production with integrated microchannel fuel processor for portable fuel cell systems, J. Power Sources 145 (2005) 702–706.

[4] G. Chen, Q. Yuan, H. Li, S. Li, CO selective oxidation in a microchannel reactor for PEM fuel cell, Chem. Eng. J. 101 (2004) 101–106.

[5] T. Henning, J.J. Brandner, K. Schubert, Characterisation of electrical ly powered micro-heat exchangers, Chem. Eng. J. 101 (2004) 339–345.

[6] W. Ehrfeld, K. Golbig, V. Hessel, H. Lowe, T. Richter, Characterization of mixing in micromixers by a test reaction: single mixing units and mixer arrays, Ind. Eng. Chem. Res. 38 (1999) 1075–1082.

[7] J.M. Commenge, L. Falk, J.P. Corriou, M. Matlosz, Optimal design for flow uniformity in microchannel reactors, AIChE J. 48 (2002) 345–357.

[8] O. Tonomura, S. Tanaka, M. Noda, M. Kano, S. Hasebe, I. Hashimoto, CFD-based optimal design of manifold in plate-fin microdevices, Chem. Eng. J. 101 (2004) 397–402.

[9] J. Judy, D. Maynes, B.W. Webb, Characterization of frictional pressure drop for liquid flows through microchannels, Int. J. Heat Mass Transfer. 45 (2002) 3477–3489.

[10] C. Amador, A. Gavriilidis, P. Angeli, Flow distribution in different microreactor scale-out geometries and the effect of manufacturing tolerances and channel blockage, Chem. Eng. J. 101 (2004) 379–390.